



## UvA-DARE (Digital Academic Repository)

### BeppoSAX Serendipitous Discovery of the X-Ray Pulsar SAX J1802.7-2017

Augello, G.; Iaria, R.; Robba, N.R.; di Salvo, T.; Burderi, L.; Lavagetto, G.; Stella, L.

**DOI**

[10.1086/379092](https://doi.org/10.1086/379092)

**Publication date**

2003

**Published in**

Astrophysical Journal

[Link to publication](#)

**Citation for published version (APA):**

Augello, G., Iaria, R., Robba, N. R., di Salvo, T., Burderi, L., Lavagetto, G., & Stella, L. (2003). BeppoSAX Serendipitous Discovery of the X-Ray Pulsar SAX J1802.7-2017. *Astrophysical Journal*, 596(1), L63-L66. <https://doi.org/10.1086/379092>

**General rights**

It is not permitted to download or to forward/distribute the text or part of it without the consent of the author(s) and/or copyright holder(s), other than for strictly personal, individual use, unless the work is under an open content license (like Creative Commons).

**Disclaimer/Complaints regulations**

If you believe that digital publication of certain material infringes any of your rights or (privacy) interests, please let the Library know, stating your reasons. In case of a legitimate complaint, the Library will make the material inaccessible and/or remove it from the website. Please Ask the Library: <https://uba.uva.nl/en/contact>, or a letter to: Library of the University of Amsterdam, Secretariat, Singel 425, 1012 WP Amsterdam, The Netherlands. You will be contacted as soon as possible.

*BeppoSAX* SERENDIPITOUS DISCOVERY OF THE X-RAY PULSAR SAX J1802.7–2017

G. AUGELLO,<sup>1</sup> R. IARIA,<sup>1</sup> N. R. ROBBA,<sup>1</sup> T. DI SALVO,<sup>1,2</sup> L. BURDERI,<sup>3</sup> G. LAVAGETTO,<sup>1</sup> AND L. STELLA<sup>3</sup>

Received 2003 June 18; accepted 2003 August 15; published 2003 September 17

ABSTRACT

We report on the serendipitous discovery of a new X-ray source, SAX J1802.7–2017,  $\sim 22'$  away from the bright X-ray source GX 9+1, during a *BeppoSAX* observation of the latter source on 2001 September 16–20. SAX J1802.7–2017 remained undetected in the first 50 ks of observation; the source count rate in the following  $\sim 300$  ks ranged between 0.04 and 0.28 counts  $s^{-1}$ , corresponding to an averaged 0.1–10 keV flux of  $3.6 \times 10^{-11}$  ergs  $cm^{-2} s^{-1}$ . We performed a timing analysis and found that SAX J1802.7–2017 has a pulse period of 139.612 s, a projected semimajor axis of  $a_x \sin i \sim 70$  lt-s, an orbital period of  $\sim 4.6$  days, and a mass function  $f(M) \sim 17 \pm 5 M_\odot$ . The new source is thus an accreting X-ray pulsar in a (possibly eclipsing) high-mass X-ray binary. The source was not detected by previous X-ray astronomy satellites, indicating that it is likely a transient system.

*Subject headings:* pulsars: general — pulsars: individual (SAX J1802.7–2017) — stars: magnetic fields — stars: neutron — X-rays: binaries

1. INTRODUCTION

High-mass X-ray binaries (HMXBs) are young systems, and the neutron stars (NSs) that are often hosted in them usually have a strong magnetic field ( $B \sim 10^{12}$  G). Accretion onto these NSs occurs via capture of stellar wind matter and Roche lobe overflow. HMXBs comprise two main subgroups: (1) the supergiant systems and (2) the Be star systems. In the supergiant systems, the companion is of spectral type earlier than B2 and has evolved off the main sequence. Orbital periods are generally less than 10 days, orbits are circular, and the mass transfer takes place because of the strong stellar wind from the OB star and/or because of “incipient” Roche lobe overflow. The Be star systems are characterized by emission lines (mainly the Balmer series) that originate in the equatorial circumstellar envelope of the companion star. The orbital periods in these systems tend to be longer than those of group 1 and correlate well with the pulsar spin period (Corbet 1986). The orbits are usually moderately eccentric. Transient activity is common in Be HMXBs; different types of outburst have been observed from different sources and occasionally also from the same source. Giant outbursts involve high peak luminosities, occur at any orbital phase, and show only little (if any) orbital modulation of the X-ray flux. Recurrent outbursts usually involve lower peak luminosities, tend to occur close to periastron, and sometimes show a strong modulation of the X-ray flux with the orbital phase (see, e.g., Stella, White, & Rosner 1986). To date, about 80 HMXBs are known;  $\sim 40$  of them show periodic X-ray pulsations with spin periods distributed over a wide range from 69 ms to  $\sim 24$  minutes (see Nagase 1989 for a review).

While studying the atoll source GX 9+1 with *BeppoSAX*, we have discovered a new X-ray pulsator in an HMXB. We report here the results of the timing analysis of this new X-ray source.

2. OBSERVATIONS

The observation of the GX 9+1 field was carried out from 2001 September 16 (02:01:30.0 UTC) to 2001 September 20 (03:00:08.5 UTC), using the co-aligned Narrow Field Instruments (NFIs) on board *BeppoSAX*: a Low Energy Concentrator Spectrometer (LECS; energy range 0.1–10 keV; Parmar et al. 1997), two Medium Energy Concentrator Spectrometers (MECSs; energy range 1–10 keV; Boella et al. 1997), a High Pressure Gas Scintillation Proportional Counter (HPGSPC; energy range 7–60 keV; Manzo et al. 1997), and a Phoswich Detector System (PDS; energy range 13–200 keV; Frontera et al. 1997). The exposure times were  $\sim 60$ ,  $\sim 149$ ,  $\sim 142$ , and  $\sim 71$  ks for LECS, MECS, HPGSPC, and PDS, respectively. The circular field of view (FOV) of the LECS and MECS is  $37'$  and  $56'$  in diameter, respectively, while those of the HPGSPC and PDS are hexagonal with FWHMs of  $78'$  and  $66'$ , respectively. The LECS and MECS detectors are position-sensitive counters with imaging capability. The position reconstruction uncertainty for MECS is  $0.5$  in the central area of  $9'$  radius and  $\sim 1.5$  in the outer region of the FOV (Boella et al. 1997). The HPGSPC and PDS systems do not have imaging capabilities, and their data are therefore difficult to interpret and analyze for individual sources when the FOV includes more than one source.

Figure 1 shows the *BeppoSAX*/MECS image (1–10 keV) centered at the position of the bright atoll source GX 9+1. A fainter source is visible at R.A. (2000.0) =  $18^{\circ}02^m39^s.9$  and decl. (2000.0) =  $-20^{\circ}17'13''.50$  (position uncertainty  $2''$ ), at an angular distance from GX 9+1 of  $\sim 22'$ . The source was outside the FOV of the *BeppoSAX*/LECS. We have verified its presence in both the MECS2 and MECS3 images, which probably excludes that this was a ghost image of a source outside the MECS FOV. Moreover, we can be sure that the source was within the PDS FOV because the source X-ray pulsations were also detected in the PDS data (see below). We searched for known X-ray sources in a circular region of  $30'$  centered at GX 9+1 in the SIMBAD database. We found no known sources with a position compatible with that of the faint source; we therefore designate this serendipitous source as SAX J1802.7–2017.

We extracted the MECS events of SAX J1802.7–2017 from an elliptical region centered at R.A. (2000.0) =  $18^{\circ}02^m39^s.9$  and decl. (2000.0) =  $-20^{\circ}17'13''.50$  and the background events from an elliptical region similar to the one used for the source,

<sup>1</sup> Dipartimento di Scienze Fisiche ed Astronomiche, Università di Palermo, via Archirafi 36, I-90123 Palermo, Italy; augello@gifco.fisica.unipa.it, iaria@gifco.fisica.unipa.it, robba@gifco.fisica.unipa.it.

<sup>2</sup> Astronomical Institute “Anton Pannekoek,” University of Amsterdam and Center for High-Energy Astrophysics, Kruislaan 403, NL 1098 SJ Amsterdam, Netherlands; disalvo@science.uva.nl.

<sup>3</sup> Osservatorio Astronomico di Roma, via Frascati 33, I-00040 Monteporzio Catone (Rome), Italy; burderi@mporzio.astro.it, stella@mporzio.astro.it.

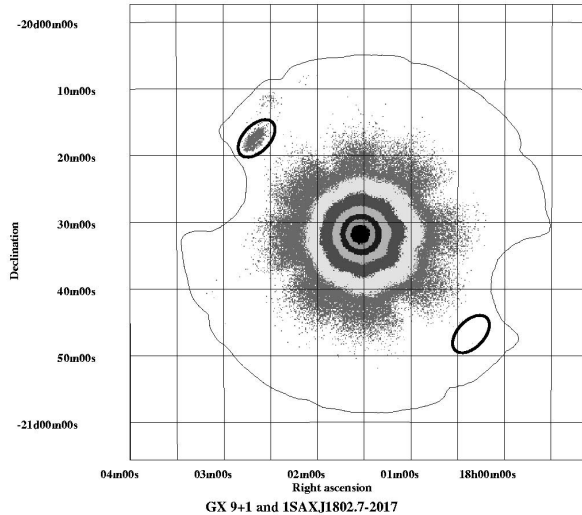


FIG. 1.—*BeppoSAX*/MECS image (1–10 keV) of the GX 9+1 field. SAX J1802.7–2017 is visible at the top left. Its angular separation from GX 9+1 is  $\sim 22'$ . The extraction region of the source and background are also shown. The two semicircular “cutouts” are due to the removal of internal calibration source events.

centered at a symmetric position with respect to the center of the MECS FOV and not contaminated by GX 9+1 (see Fig. 1). In Figure 2, the light curves of SAX J1802.7–2017 plus background (*crosses*) and of the background (*asterisks*) are shown. The source was not detected during the first 50 ks when the count rate within the extraction region ( $0.034 \pm 0.001$  counts  $s^{-1}$ ) was compatible with the background count rate. In the following  $\sim 300$  ks, the source count rate showed a large variability with an average intensity significantly above the background level. Two flaring events took place  $\sim 110$  and  $\sim 300$  ks from the beginning of the observation.

### 3. TEMPORAL ANALYSIS

The arrival time of all events in the MECS and PDS were corrected to the solar system barycenter. We searched for periodicities by computing a power spectrum density (PSD) in the range between  $4 \times 10^{-4}$  Hz and 1 kHz from fast Fourier transforms performed on MECS data of SAX J1802.7–2017.

A main peak at a frequency of  $\sim 7.20$  mHz, corresponding to a period of  $\sim 139$  s, is evident (see Fig. 3). The second harmonic is also clearly visible. We performed a folding search for periods centered around  $\sim 139$  s, finding a not well-defined period, because two  $\chi^2$  peaks were present at  $\sim 139.49$  and  $\sim 139.70$  s, respectively.

To study possible delays in the pulse arrival times or, equivalently, pulse period variations, we divided the whole data set into 35 consecutive intervals each having a length of about 10 ks. We found that only 27 of these intervals had enough statistics to carry out the analysis described below. A folding search was performed in each interval for a range of trial periods centered around 139 s. The corresponding best periods were obtained by fitting the  $\chi^2$  versus trial period curve with a Gaussian function. The best periods varied significantly and with continuity between 139.44 and 139.86 s with an average value of 139.608 s.

Phase delays (Fig. 4) were obtained by cross-correlating the folded light curves obtained for each of the 27 intervals with that of the whole observation used as a template (an average

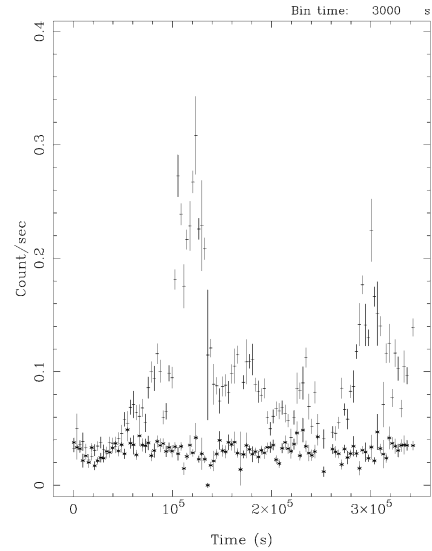


FIG. 2.—MECS light curves (1–10 keV) of SAX J1802.7–2017 plus background (*crosses*) and of the background (*asterisks*). The bin time is 3000 s.

pulse period of 139.608 s was adopted in the folding). Initially we fitted the phase delays  $\Delta\phi$  using

$$\Delta\phi = a_0 + a_1 t_n + a_2 t_n^2, \quad (1)$$

where  $t_n$  is the arrival time of the  $n$ th pulse. In this formula, the linear term  $a_1 = \Delta P_{\text{pulse}}/P_{\text{pulse}}^2$  and the quadratic term  $a_2 = \dot{P}_{\text{pulse}}/2P_{\text{pulse}}^2$  are related to a correction to the pulse period and the derivative of the pulse period, respectively. We obtained a  $\chi_{\text{red}}^2$  of 2.6, indicating that the modulation of the phase delays cannot only be explained by the presence of a derivative of the pulse period. Moreover, we find a value of  $\dot{P}_{\text{pulse}}/P_{\text{pulse}}$  of  $0.40 \pm 0.01 \text{ yr}^{-1}$ , more than an order of magnitude larger than the largest measured value in any known X-ray pulsar (i.e.,  $-10^{-2} \text{ yr}^{-1}$  in GX 1+4; see Pereira, Braga, & Jablonski 1999).

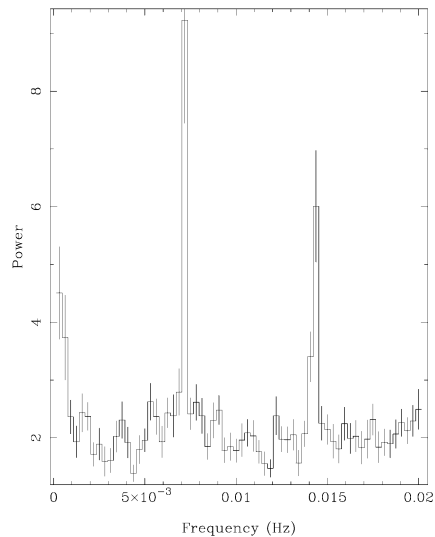


FIG. 3.—PSD of SAX J1802.7–2017 obtained from MECS data (1.0–10.5 keV energy band) extracted from an elliptical region centered on the source, as described in the text. Sixty-one PSDs, computed from time intervals of  $\sim 5$  ks length, were averaged. The fundamental harmonic and the second harmonic are clearly visible at 7.2 and 14.4 mHz, respectively. The PSD is normalized according to the prescription of Leahy et al. (1983).

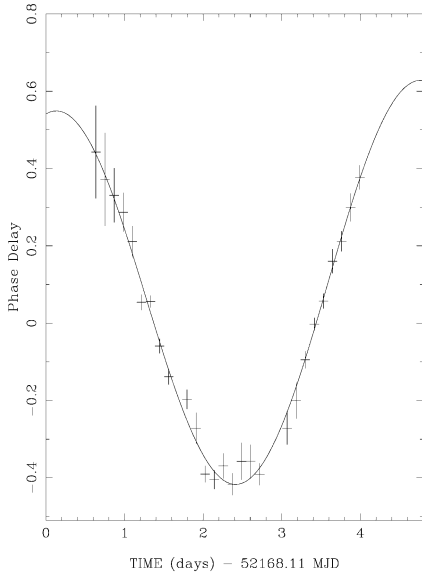


FIG. 4.—Phase delays of SAX J1802.7–2017 as a function of time. The solid line is the best-fit function (eq. [2]) discussed in the text; the orbital period is  $\sim 4.6$  days.

We checked whether the modulation of the phase delays could be explained by the propagation delays due to the orbital motion of the X-ray pulsar around a companion star by fitting the phases with

$$\Delta\phi = a_0 + a_1 t_n + B \cos \left[ \frac{2\pi(t_n - T_{\pi/2})}{P_{\text{orb}}} \right]. \quad (2)$$

The results of the fit are reported in Table 1. The  $\chi^2_{\text{red}}$  was 1.3. Since  $a_x \sin i = P_{\text{pulse}} B$ , we find  $a_x \sin i \sim 70$  lt-s; the corrected pulse period was  $\sim 139.612$  s.

We tried to add a quadratic term to equation (2) to take into account a spin period derivative but because of the small number of points and a relatively short observation, we could not constrain all parameters of the fit. In any case, by fixing the quadratic term in the range from  $-9 \times 10^{-3}$  to  $9 \times 10^{-3} \text{ day}^{-2}$  (corresponding to a  $\dot{P}_{\text{pulse}}/P_{\text{pulse}}$  in the range from  $-10^{-2}$  to  $10^{-2} \text{ yr}^{-1}$ ), we found that the orbital parameters do not change significantly ( $\sim 2\%$  changes in the orbital period value, and  $\sim 4\%$  in the  $a_x \sin i$  value) with respect to the parameters reported in Table 1.

We corrected the arrival times of all the events, observed by the MECS and PDS instruments, to the center of mass of the binary system using the orbital parameters and the corrected pulse period reported in Table 1. We then recomputed, on the corrected folded light curves, the phase delays and found that they are compatible with zero phase delay (see Fig. 5). This suggests that our data are compatible with a circular orbit, although an eccentricity could be present but not appreciated because of the relatively low statistics of our data. To estimate a rough upper limit to the eccentricity of the system, we fitted our phase delays, substituting the circular orbital correction in equation (2) with a first-order approximation of the eccentric orbital correction (see, e.g., van der Klis & Bonnet-Bidaud 1984), thus obtaining  $e \lesssim 0.2$  (90% confidence level) and  $\chi^2_{\text{red}} \sim 1.4$ .

Using the estimated pulse period, we folded the MECS light curves in the energy bands 1–3, 3–6, and 6–10 keV, and the PDS light curves in the energy bands 13–25 and 25–80 keV,

TABLE 1  
ORBITAL PARAMETERS OF SAX J1802.7–2017

Parameter	Value
$a_0$ .....	$0.04^{+0.12}_{-0.09}$
$a_1$ .....	$0.02 \pm 0.03 \text{ day}^{-1}$
$B$ .....	$0.50^{+0.07}_{-0.05}$
$P_{\text{orb}}$ .....	$4.6^{+0.4}_{-0.3} \text{ days}$
$a_x \sin i$ .....	$70^{+10}_{-7} \text{ lt-s}$
$T_{\pi/2}$ .....	$52,168.22^{+0.10}_{-0.12} \text{ MJD}$
$P_{\text{pulse}}$ .....	$139.612^{+0.006}_{-0.007} \text{ s}$

NOTE.—Errors are at the 1  $\sigma$  confidence level.

excluding the first 50 ks of our observation. The main pulse of the modulation presents a peak around phase 0.6. A secondary peak is visible around phase 0.1, which appears to be more prominent at higher energies. The pulse fraction, defined as  $(I_{\text{max}} - I_{\text{min}})/I_{\text{max}}$ , with  $I_{\text{max}}$  and  $I_{\text{min}}$  the maximum and minimum count rate, are  $43\% \pm 7\%$ ,  $57\% \pm 6\%$ ,  $62\% \pm 8\%$ ,  $7\% \pm 2\%$ , and  $36\% \pm 3\%$  in the 1–3, 3–6, 6–10, 13–25, and 25–80 keV energy band, respectively. The pulse fraction in the 13–25 and 25–80 keV energy bands is strongly reduced by the presence of GX 9+1 in the PDS FOV (note, however, that the pulse fraction between 25 and 80 keV is somewhat higher because GX 9+1 is weaker at these energies). In Figure 6, we show the folded light curves in the energy bands 1–3, 3–6, 6–10, and 25–80 keV.

#### 4. DISCUSSION

We have discovered a serendipitous source, SAX J1802.7–2017, in a *BeppoSAX*/NFI observation of the bright atoll source GX 9+1. SAX J1802.7–2017 shows coherent pulsations at a period of 139.612 s, indicating that the compact object in this system is most likely an accreting magnetic NS. Pulse arrival times show a sinusoidal modulation at a period of 4.6 days, which we interpret as being due to the orbital motion of the source. The values of the orbital period and of the pulse period, as well as the pulse fraction in the MECS energy range ( $\sim 40\%$ – $60\%$ ), are consistent with the values usually found for HMXB systems (e.g., Oosterbroek et al. 1999; Bildsten et al. 1997).

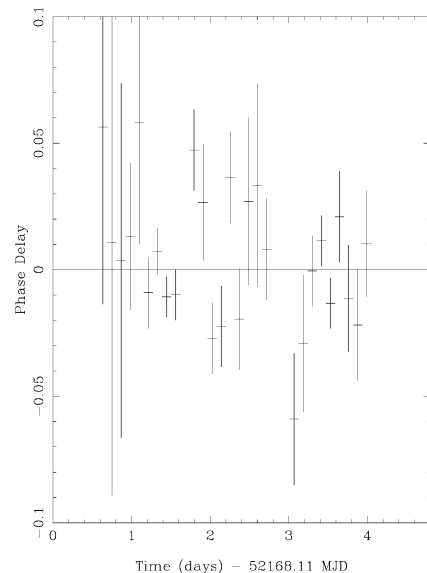


FIG. 5.—Phase delays after the barycentric correction with respect to the center of mass of the binary system.

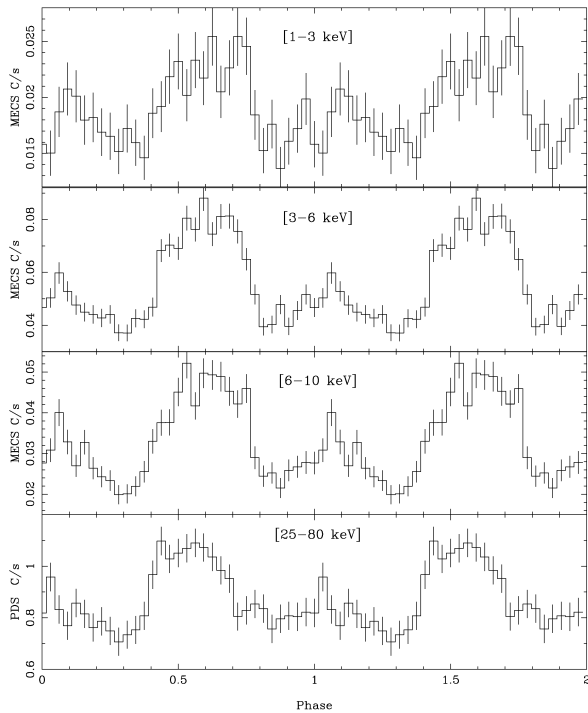


FIG. 6.—Folded light curves in four different energy bands. *From top to bottom*: 1–3, 3–6, 6–10 (MECS), and 25–80 keV (PDS). The folding is obtained for a pulse period of 139.612 s, and the zero epoch was assumed at the superior conjunction  $T_{\pi/2} = 52,168.22$  MJD.

The mass function of the system is

$$f(M) = \frac{M_C \sin^3 i}{(1+q)^2} = \left(\frac{2\pi}{P_{\text{orb}}}\right)^2 \frac{(a_x \sin i)^3}{G} \sim 17 \pm 5 M_{\odot},$$

where  $M_C$  is the companion star mass,  $G$  is the gravitational constant, and  $q$  is the ratio of the compact object mass to the companion mass. The value of the mass function is not compatible with the system being a cataclysmic variable in which a white dwarf is orbiting an  $\sim 1 M_{\odot}$  companion. For an NS mass of  $1.4 M_{\odot}$ , we have estimated a lower limit on the companion star mass,  $M_C \gtrsim 11 M_{\odot}$  (90% confidence level), typical of an HMXB. The epoch of the NS superior conjunction (which would correspond to the mideclipse time) derived from the fit of the orbital parameters falls during the first 50 ks of our observation, when the count rate of SAX J1802.7–2017 is compatible with the background count rate. This is compatible with the possible presence of an eclipse during the first 50 ks. Assuming that the eclipse ends  $\sim 0.58$  days after the beginning of our observation (52,168.69 MJD; see Fig. 2) and taking into account that the zero epoch is  $0.11 \pm 0.10$  days, the half-

duration of the eclipse should be  $0.47 \pm 0.10$  days. The half-angle of the eclipse subtending the portion of circular orbit covered by the source is  $\theta = 0.64 \pm 0.14$  rad. The eclipse duration is related to the inclination angle  $i$  of the system by  $R_C/a = (\cos^2 i + \sin^2 i \sin^2 \theta)^{1/2}$ , where  $R_C$  is the radius of a spherical primary star and  $a$  is (approximately) the separation between the two stars (see Primini et al. 1976). Then a rough lower limit on the companion star radius is  $R_C \gtrsim 14 R_{\odot}$ .

To estimate the luminosity of the source, we performed a spectral analysis in the MECS range using the correct effective area for the position of the source in the MECS FOV (G. Cusumano 2003, private communication). Although the low statistics of the data did not allow an accurate spectral analysis, we inferred a luminosity of  $\sim 5.6 \times 10^{35}$  ergs  $s^{-1}$  over the 1.8–10 keV range by fitting the data to a power law (photon index  $-0.1 \pm 0.1$  and  $N_H = 1.7^{+0.8}_{-0.9} \times 10^{22}$   $\text{cm}^{-2}$ ) and assuming a source distance of 10 kpc. The light curve of the system shows a large variability, suggesting that the system could be accreting via a stellar wind. This is also suggested by its long pulse period and relatively short orbital period, typical of HMXBs accreting via stellar wind such as Vela X-1 and 4U 1538–52 (see, e.g., Corbet 1986 and Nagase 1989). Indeed, SAX J1802.7–2017 shows similarities to 4U 1538–52, which has a long spin period of  $\sim 529$  s, a short orbital period of  $\sim 3.7$  days, and a mass of  $19.8 \pm 3.3 M_{\odot}$  for the companion star (Reynolds, Bell, & Hilditch 1992). However, while the averaged luminosity of 4U 1538–52 and Vela X-1 is around  $5 \times 10^{36}$  ergs  $s^{-1}$ , the averaged luminosity of SAX J1802.7–2017 measured during our observation is at least 1 order of magnitude lower (assuming an upper limit to the distance of 10 kpc). The source seems therefore to be quite underluminous with respect to massive binaries accreting via stellar wind, although more observations are needed to confirm this conclusion.

Note that since the source has not been reported by other X-ray astronomy satellites (in particular, we did not find any detected source at the position of SAX J1802.7–2017 in *ROSAT* images, although the field of GX 9+1 was not observed by *ASCA*), it might well be a transient HMXB. Most of the transient HMXBs are Be star systems (Liu, van Paradijs, & van den Heuvel 2000). However, if SAX J1802.7–2017 belongs to this class, it should be atypical considering that its orbital period and pulse period do not follow the Corbet correlation (Corbet 1986). Note also that the presence of an eccentricity cannot be excluded by our data, and more observations are needed to confirm the orbital parameters of the source.

We thank Giancarlo Cusumano for providing us with the corrected effective area for our source and the anonymous referee for useful suggestions. This work was partially supported by the Italian Space Agency (ASI), by the Ministero della Istruzione, della Università e della Ricerca (MIUR), and by the Netherlands Organization for Scientific Research (NWO).

#### REFERENCES

- Bildsten, L., et al. 1997, *ApJS*, 113, 367  
 Boella, G., Butler, R. C., Perola, G. C., Piro, L., Scarsi, L., & Bleeker, J. A. M. 1997, *A&AS*, 122, 299  
 Corbet, R. H. D. 1986, *MNRAS*, 220, 1047  
 Frontera, F., Costa, E., dal Fiume, D., Feroci, M., Nicastro, L., Orlandini, M., Palazzi, E., & Zavattini, G. 1997, *A&AS*, 122, 357  
 Leahy, D. A., Darbro, W., Elsner, R. F., Weisskopf, M. C., Kahn, S., Sutherland, P. G., & Grindlay, J. E. 1983, *ApJ*, 266, 160  
 Liu, Q. Z., van Paradijs, J., & van den Heuvel, E. P. J. 2000, *A&AS*, 147, 25  
 Manzo, G., Giarrusso, S., Santangelo, A., Ciralli, F., Fazio, G., Piraino, S., & Segreto, A. 1997, *A&AS*, 122, 341  
 Nagase, F. 1989, *PASJ*, 41, 1  
 Oosterbroek, T., et al. 1999, *A&A*, 351, L33  
 Parmar, A. N., et al. 1997, *A&AS*, 122, 309  
 Pereira, M. G., Braga, J., & Jablonski, F. 1999, *ApJ*, 526, L105  
 Primini, F., Clark, G. W., Lewin, W., Li, F., Mayer, W., McClintock, J., Rapaport, S., & Joss, P. C. 1976, *ApJ*, 210, L71  
 Reynolds, A. P., Bell, S. A., & Hilditch, R. W. 1992, *MNRAS*, 256, 631  
 Stella, L., White, N. E., & Rosner, R. 1986, *ApJ*, 308, 669  
 van der Klis, M., & Bonnet-Bidaud, J. M. 1984, *A&A*, 135, 155